ISSN 0965-5441, Petroleum Chemistry, 2018, Vol. 58, No. 12, pp. 1023–1031. © Pleiades Publishing, Ltd., 2018.
Original Russian Text © O.A. Ponomareva, P.A. Shaposhnik, P.A. Kots, S.V. Konnov, B.A. Kolozhvari, I.I. Ivanova, 2018, published in Neftekhimiya, 2018, Vol. 58, No. 6, pp. 677–685.

Synthesis of Isobutylene from Ethanol in the Presence of Catalysts Containing Zinc Oxide and Zirconia

O. A. Ponomareva[a, b, *], **P. A. Shaposhnik**[b], **P. A. Kots**[b], **S. V. Konnov**[a],
B. A. Kolozhvari[a, b], **and I. I. Ivanova**[a, b]

[a] *Topchiev Institute of Petrochemical Synthesis, Russian Academy of Sciences, Moscow, Russia*
[b] *Faculty of Chemistry, Moscow State University, Moscow, Russia*
**e-mail: oaponomareva@phys.chem.msu.ru*

Received June 15, 2018

Abstract—Synthesis of isobutylene from ethanol in the presence of ZnO/ZrO_2 catalysts has been studied. The samples have been synthesized by incipient wetness impregnation of zirconium hydroxide derived from zirconyl chloride with zinc nitrate and subsequent calcination at 550°C. The synthesized samples have been studied by low-temperature nitrogen adsorption, SEM, XRD, IR spectroscopy of adsorbed CO, and TGA–DTA. Studies of the effect of the catalyst composition and the test conditions have revealed that, during the synthesis of isobutylene from ethanol, an optimum Zr : Zn molar ratio providing the production of isobutylene with a selectivity of 45–50% is 8–20 and optimum conditions for ethanol conversion to isobutylene are 500°C, a feed space velocity of 3 g/(g h), and a feedstock in the form of a 50% ethanol solution in water. According to thermogravimetric analysis, an increase in the zinc content in the samples leads to a decrease in the amount of coke deposits.

Keywords: ethanol, isobutylene, zinc oxide, zirconia, incipient wetness impregnation

DOI: 10.1134/S0965544118120113

Bioethanol, which is one of the most readily available renewable resources derived by plant matter fermentation, is a feedstock for synthesizing a wide range of products, such as ethylene [1–4], aromatic hydrocarbons [2], propylene [1, 5–8], isobutylene [9–13], butadiene [14], butanol [3, 15], ethyl acetate [16, 17], hydrogen [18], acetone [3, 17, 19, 20], acetaldehyde [15, 17], and acetic acid [21]. One of the most promising ethanol-based processes is the single-stage synthesis of isobutylene [8–13]. Isobutylene, which is a feedstock for large-scale processes aimed at the production of methyl methacrylate, polymers, and methyl *tert*-butyl ether [22], is currently produced by oil refining. Since the demand for isobutylene is constantly increasing, while the oil reserves are being depleted, an urgent problem is to develop alternative isobutylene synthesis methods to decrease the dependence of the production on fossil natural resources and hydrocarbon market fluctuations.

Isobutylene has been first synthesized from ethanol by Wang et al. in the presence of a $Zn_xZr_yO_z$ mixed bifunctional oxide catalyst prepared by the hard template-assisted synthesis [9]. It was found that a key role in the production of isobutylene is played by Lewis acid–base pairs, whereas the presence of Brønsted acid sites (BASs) contributes to the occurrence of side reactions, namely, isobutylene isomerization, butene oligomerization, and coke formation [10]. Synthesis of $Zn_xZr_yO_z$ by incipient wetness impregnation of zirconium hydroxide with zinc salt solutions provides the formation of catalysts characterized by the presence only of Lewis acid–base sites; this feature contributes to an increase in the stable on-stream time of the catalysts [10]. Studies of the effect of the composition of the zinc salts used to synthesize the catalyst showed that an important role is played by the size of the zinc salt anion. The most active catalyst was obtained using zinc acetate [12]. The authors of that study attribute this finding to the fact that $Zn_xZr_yO_z$ synthesized by impregnation with zinc acetate is characterized by an optimum balance of acid and base sites, a high degree of dispersion of zinc, and a stronger interaction of the metal oxide with the substrate. Recently, An et al. have published data on the synergistic effect of chromium additives to a $Zn_xZr_yO_z$ catalyst prepared by a template-assisted technique in the synthesis of isobutylene from ethanol [13].

Despite the fact that the synthesis of $Zn_xZr_yO_z$ catalysts by incipient wetness impregnation of zirconium hydroxide with zinc salts is simpler, more adaptable to streamlined production, and cheaper, most of the reports are focused on $Zn_xZr_yO_z$ prepared by hard template-assisted synthesis [9–11, 13]. There are no published data on the effect of the composition of

$Zn_xZr_yO_z$ catalysts synthesized by incipient wetness impregnation on the catalytic properties of these samples and no data on thermogravimetric and differential thermal analysis (TGA–DTA) of the samples coked during the synthesis of isobutylene from ethanol.

This study is focused on ethanol conversion to isobutylene in the presence of $Zn_xZr_yO_z$ catalysts that are synthesized by incipient wetness impregnation of zirconium hydroxide with a zinc nitrate solution and contain different amounts of zinc oxide and zirconia; the effect of reaction conditions on the process parameters is determined; the deactivated catalysts of different compositions are studied by TGA–DTA.

EXPERIMENTAL

Catalysts based on zirconia modified with zinc compounds were studied in the synthesis of isobutylene from ethanol; the catalysts were prepared by incipient wetness impregnation of zirconium hydroxide derived from $ZrOCl_2 \cdot 8H_2O$ by precipitation with a 5 M NaOH solution to provide the Zn : Zr ratio in the resulting catalyst of 1 : 2, 1 : 6, 1 : 8, 1 : 14, 1 : 20, and 1 : 40 and subsequent calcination at 550°C. In addition, for comparison, original ZrO_2 was synthesized by the calcination of zirconium hydroxide derived from $ZrOCl_2 \cdot 8H_2O$ by precipitation with a 5 M NaOH at 550°C for 6 h.

The chemical composition of the samples was determined by X-ray fluorescence analysis on a Thermo Scientific ARL Perform`X instrument equipped with a 3.5-kW rhodium tube.

The surface morphology of the synthesized samples was studied by scanning electron microscopy (SEM) on a Hitachi Tabletop Microscope TM3030Plus electron microscope. The voltage across the accelerating electrode was 15 kV; the used magnifications were ×500 to 20000.

Characteristics of the pore structure of the catalysts were studied on a Micrometrics ASAP 2000 automatic sorption meter.

X-ray diffraction patterns (XRD analysis) were recorded at room temperature on a Bruker D2 PHASER powder diffractometer in the θ–θ geometry. The generator mode was 30 kV and 10 mA; an X-ray tube with a copper anode was used ($CuK_{\alpha 1}$ radiation, λ = 1.5418 Å). Diffraction patterns were recorded while rotating samples in a horizontal plane in a 2θ angular range of 5°–50° in increments of 0.05°; the slit width at the outlet of the tube and in front of the detector was 0.6 and 1.15 mm, respectively; the acquisition time was 3 s per point. The diffraction patterns were processed using the Bruker DIFFRAC.EVA software package. Phases were identified in accordance with the ICDD PDF2 database.

Infrared spectra were recorded on a Nicolet Protege 460 Fourier transform IR spectrometer equipped with an MCT detector in a range of 4000–400 cm^{-1} with a resolution of 4 cm^{-1}. A 20-mg catalyst sample was compressed into a disc with a diameter of 2 cm at a pressure of 100 atm. Water was removed from the samples on a vacuum unit equipped with absolute pressure sensors with a working vacuum of 5×10^{-4} Pa. A pellet of the sample was placed in an IR cell, heated to 450°C for 2 h, and held at 450°C for 1 h. Carbon monoxide adsorption was conducted at the liquid nitrogen temperature (77 K) by dosing the gas until complete saturation. The recorded IR spectra were processed using the OMNIC ESP software, version 7.3.

The deactivated samples were studied by TGA–DTA on a NETZSCHSTA 409 PC/PG instrument combined with a mass spectrometer. Analysis was conducted using 20–30 mg of the sample. The sample was heated in a dry air stream (100 mL/min) from room temperature to 800°C at a rate of 10°C/min.

Catalytic tests were conducted in a flow reactor at atmospheric pressure in a temperature range of 440–500°C at space velocities of the feedstock (50% ethanol solution in water) of 1.3–14.5 g/(g h) in the presence of nitrogen (10 mL/min). The feedstock composition was varied by varying the ethanol content in water from 20 to 80 wt %. Nitrogen and dioxane were used as the internal standard for gases and liquid samples, respectively.

Liquid and gaseous reaction products were analyzed on a Kristall 2000M gas–liquid chromatograph equipped with a flame ionization detector using nitrogen as the carrier gas and a 30 m quartz capillary column coated with the SE-30 nonpolar liquid phase. The amount of CO_2 was determined on a Kristall 2000M gas–liquid chromatograph equipped with a thermal conductivity detector using hydrogen as the carrier gas and a 3 m packed column with the Porapak-Q phase. Isobutylene and butadiene were separated on a Kristall 5000.2 chromatograph equipped with a flame ionization detector using hydrogen as the carrier gas and a 25 m quartz capillary column with the KCl/Al_2O_3 phase. Reaction products were identified on a Thermo Trace GC Ultra chromatograph combined with a Thermo DSQ II mass spectrometer using a 50 m quartz capillary column with the Ultra 1 nonpolar liquid phase.

Catalyst activity was characterized according to ethanol conversion and reaction product selectivity. Ethanol conversion, selectivities, and target product yields were calculated using results of chromatographic analysis.

Ethanol conversion (K) and ith product selectivity were calculated by the following formulas:

$$K = (m_{\text{fed ethanol}} - m_{\text{unreacted ethanol}}) \times 100 / m_{\text{fed ethanol}}, \%$$

$$S_i = 100 \times (k_i Q_i / M_{ri}) / m_{\text{reacted ethanol}}, \%$$

$$Y_i = K S_i / 100, \%$$

$$Y_{\text{with respect to theor.}} = Y_i / 100 \times Y_{\text{theor.}}, \%,$$

Table 1. Physicochemical properties of the samples

Sample	Zn : Zr ratio, mol/mol	ZnO content, wt %	S_{BET}, m^2/g	V_{pore}, cm^3/g	D_{pore}, Å
$ZnO/2ZrO_2$	1 : 2	24.5	34	0.039	46
$ZnO/6ZrO_2$	1 : 6	10.0	36	0.042	53
$ZnO/8ZrO_2$	1 : 8	7.6	35	0.048	55
$ZnO/14ZrO_2$	1 : 14	4.5	32	0.046	57
$ZnO/20ZrO_2$	1 : 20	3.2	42	0.065	62
$ZnO/40ZrO_2$	1 : 40	1.6	33	0.055	66
ZrO_2	0	0	44	0.099	91

where S_i is the weight fraction of the ith product, M_{ri} is the molecular weight of the ith product, $m_{\text{fed ethanol}}$ is the weight of ethanol fed within 1 h, $m_{\text{unreacted ethanol}}$ is the weight of unreacted ethanol, and k_i is a coefficient taking into account the number of ethanol molecules required for the formation of the product. The yield of the ith product was calculated as follows:

$$Y_i = KS_i/100,\ \%.$$

Isobutylene yield with respect to the theoretical value was calculated as follows:

$$Y_{\text{with respect to theor.}} = Y_i/100 \times Y_{\text{theor.}},\ \%,$$

in accordance with their reaction equation

$$3C_2H_5OH + H_2O = i\text{-}C_4H_8 + 2CO_2 + 6H_2.$$

RESULTS AND DISCUSSION

Physicochemical Properties of the Catalysts

The physicochemical properties of the samples and their designations are shown in Table 1.

After calcination at 550°C, all the ZnO/ZrO_2 samples have a low specific surface area of 30–40 m^2/g and a small pore volume; the pore diameter of ZnO/ZrO_2 is approximately the same at a level of about 50–60 Å, whereas zirconia is characterized by an average pore volume of 91 Å.

Scanning electron microscopy studies of the samples showed that their morphology does not depend on the composition. A micrograph of the synthesized $ZnO/8ZrO_2$ sample is shown in Fig. 1. The samples are agglomerates of irregularly shaped particles with a broad size distribution.

X-ray diffraction data for the ZnO/ZrO_2 samples of different compositions and ZrO_2 are shown in Fig. 2. Zirconia derived by the calcination of $ZrO(OH)_2$ at 550°C is a mixture of two—tetragonal and monoclinic—phases (ICDD 50-1089, 37-1484). After the modification of $ZrO(OH)_2$ with zinc nitrate and calcination at 550°C, the $ZnO/40ZrO_2$ sample still exhibits reflections corresponding to the monoclinic phase, although their intensity is significantly lower than that in ZrO_2; with an increase in the zinc content, reflections corresponding only to the tetrag-

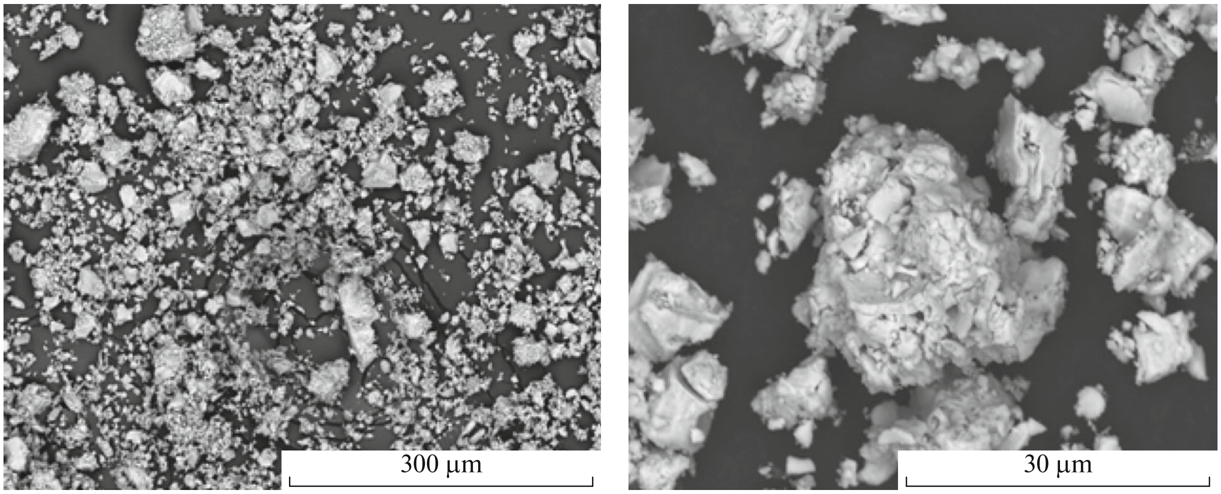

Fig. 1. Scanning electron microscopy micrographs of $ZnO/8ZrO_2$ at the different magnifications.

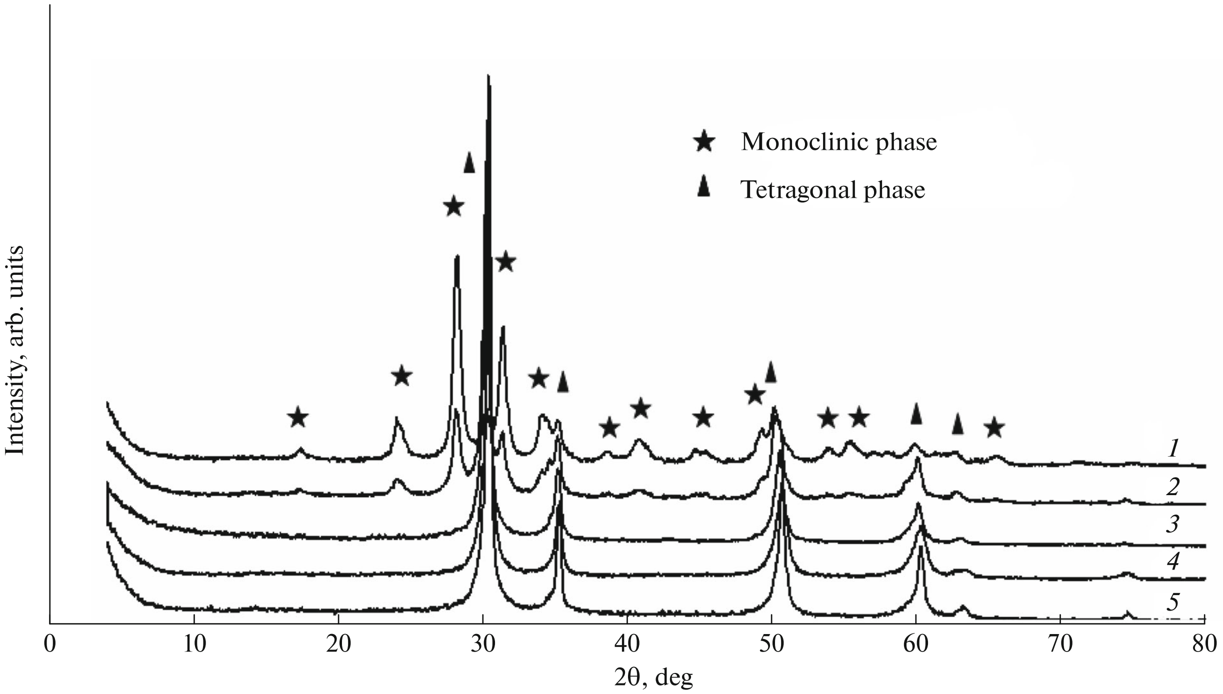

Fig. 2. Diffraction patterns of (*1*) the ZrO_2, (*2*) $ZnO/40ZrO_2$, (*3*) $ZnO/8ZrO_2$, (*4*) $ZnO/6ZrO_2$, and (*5*) $ZnO/2ZrO_2$ samples.

onal phase of zirconia were observed. This fact suggests that zinc oxide is in a highly dispersed state and hinders the tetragonal to monoclinic phase transition of ZrO_2. These results are in agreement with the data of Zavodinskii [23], who showed that doping zirconia with oxides of various metals facilitates the stabilization of zirconia in the metastable phase state.

The nature and number of acid sites were studied by IR spectroscopy of adsorbed CO. The data are shown in Fig. 3. The spectra exhibit absorption bands at 2204 cm^{-1}, which correspond to CO adsorption on Zn^{2+}; at 2154 cm^{-1}, which correspond to CO adsorption on weak BASs; and at 2168 and 2180 cm^{-1}, which correspond to CO adsorption on weak and strong Lewis acid sites (LASs), respectively. In addition, Fig. 3 shows the amount of CO adsorbed on acid sites of different strengths for ZrO_2 with different amounts of zinc oxide. It is evident that an increase in the zinc

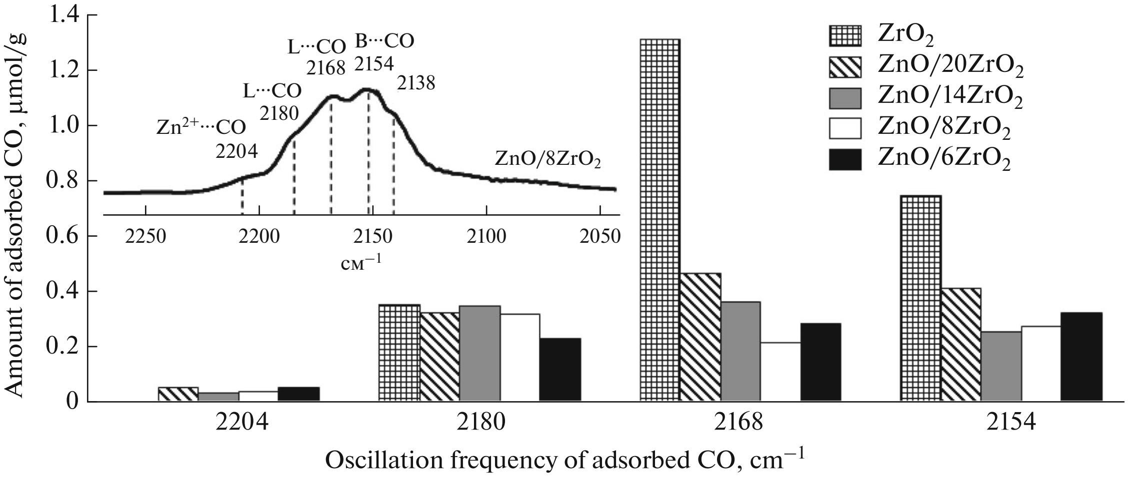

Fig. 3. Data of IR spectroscopy of adsorbed CO and the amount of CO adsorbed on acid sites of different strengths.

content has hardly any effect on the amount of CO adsorbed on zinc cations; this finding suggests that an increase in the zinc oxide content leads to the particle coarsening. An increase in the zinc content does not lead to an increase in the number of strong LASs either, whereas the amount of adsorbed CO on weak LASs and BASs decreases.

If we assume that strong LASs are located on the crystal faces, while weak LASs and BASs are located on the crystal planes, then the derived data indicate that, upon modification, zinc oxide is located on the crystal planes and thereby leads to a decrease in the number of weak LASs and BASs in ZrO_2.

Effect of Catalyst Composition on Catalytic Properties

The synthesized samples were studied in ethanol conversion to isobutylene. The reaction equation is as follows:

$$3C_2H_5OH + H_2O = i\text{-}C_4H_8 + 2CO_2 + 6H_2.$$

Ethanol conversion leads, in addition to the synthesis of the main reaction product (isobutylene), to the formation of byproducts, such as C_1–C_4 hydrocarbon gases, carbon dioxide, C_5–C_6 aliphatic hydrocarbons, isopropanol, acetone, acetaldehyde, ethyl acetate, butanal, butenal, butanone, acetic acid, pentanone, pentenone, and mesityl oxide. The assumed reaction scheme and possible routes of formation of the observed products are shown in Scheme 1.

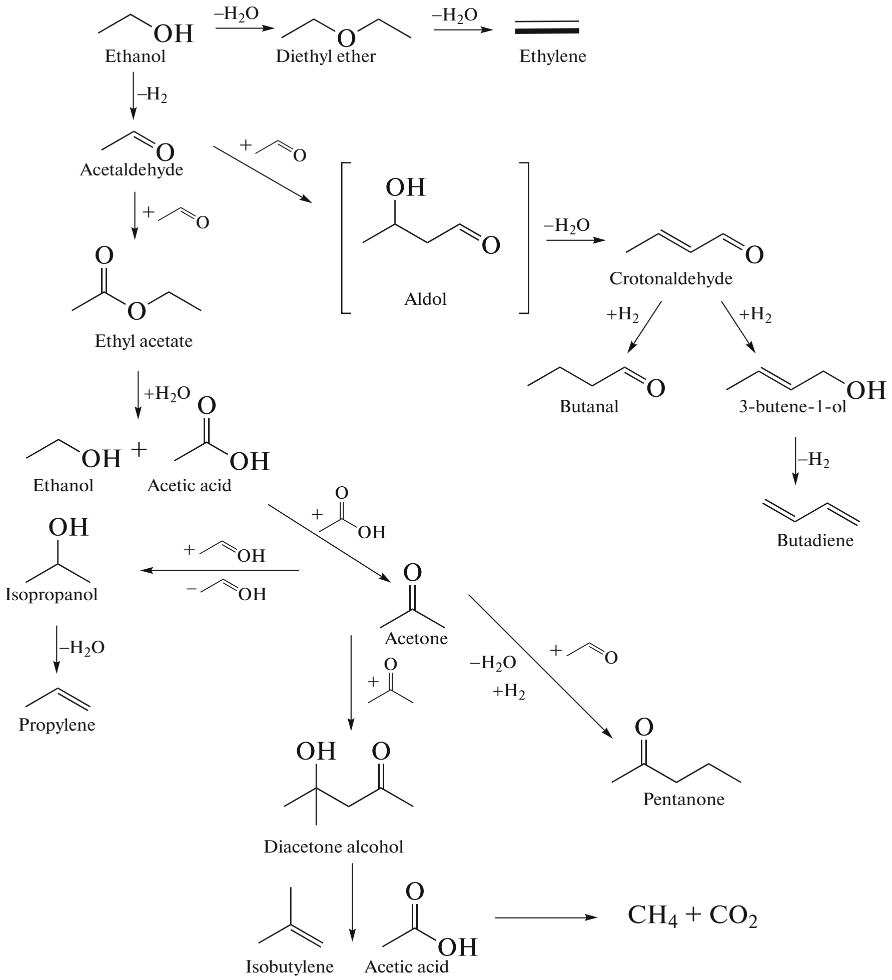

Scheme 1. Possible conversions of ethanol to isobutylene.

The catalytic conversion of ethanol to isobutylene occurs through the dehydrogenation of ethanol to acetaldehyde with subsequent disproportionation by the Tishchenko reaction to ethyl acetate, which is further hydrolyzed to acetic acid and ethanol. After that, acetic acid undergoes ketonization to form acetone, which undergoes aldol condensation to diacetone alcohol, which further forms the desired product isobutylene and acetic acid. The side reactions, i.e., dehydration, hydrogenation, condensation, isomerization, oligomerization, dehydrocyclization, etc., lead to the formation of a wide range of the observed products.

Table 2 shows results of catalytic tests on the synthesis of isobutylene from ethanol in the presence of ZnO/ZrO_2 samples of different compositions. In the presence of ZrO_2, the main reaction products are ethylene and propylene; the selectivity for these products is 79 mol %. In this case, the selectivity for the target product does not exceed 1.2%. This finding suggests that these catalysts provide the occurrence of dehydration to form ethylene. Propylene can be formed via various routes: either via the oligomerization of three ethylene molecules and subsequent metathesis or via the formation of acetone, which subsequently undergoes hydrogenation to isopropanol, which is further dehydrated to propylene. Another possible route of the formation of propylene is the condensation of two acetaldehyde molecules formed via the dehydrogenation of ethanol to 3-ol-butanal, which is further converted to butenal, which undergoes decomposition to propylene and CO. All the Zn-containing catalysts are active in the formation of isobutylene; with an increase in the zinc oxide content in the samples from 1.6 to 24.5 wt %, the isobutylene selectivity passes through a maximum. The introduction of small amounts of zinc oxide leads to an abrupt decrease in the number of weak LASs and BASs responsible for the occurrence of reactions leading to the formation of ethylene and propylene, the selectivity for which in the presence of $ZnO/20ZrO_2$ is 5 times lower than that in the case of ZrO_2. Zinc oxide mediates the dehydrogenation of ethanol to acetaldehyde, while the acid–base sites provide the occurrence of the aldolization, ketonization, and condensation reactions leading to the formation of the target product, i.e., isobutylene (Scheme 1). An increase in the zinc oxide content led to the formation of a large amount of acetone, which is apparently attributed to a decrease in the number and strength of acid sites mediating the formation of isobutylene from acetone. The optimum composition providing an isobutylene selectivity of 44–48% is the $ZnO : ZrO_2$ ratio in a range of 1 : 20 to 1 : 8; at these ratios, the isobutylene yield with respect to the theoretical value is 73–66%. Comparison of acidic (Fig. 3) and catalytic properties (Table 2) suggests that the formation of isobutylene occurs on strong LASs.

All the ZnO/ZrO_2 catalysts exhibited a stable on-stream behavior throughout the entire test, except for $ZnO/40ZrO_2$, the activity of which decreased by 20% within 2.5 h of reaction.

Effect of Reaction Conditions on the Process Parameters

Studies of the activity of the Zn–Zr-containing oxide catalysts showed that samples with a ratio of $ZnO : ZrO_2$ (Zn : Zr) = (1 : 8)–(1 : 20) are the most selective in the synthesis of isobutylene from ethanol. Therefore, the $ZnO : 8ZrO_2$ sample was selected for further studies of the effect of reaction conditions on the process parameters.

Effect of reaction temperature. In the temperature range of 440–500°C, the ethanol conversion is 100%. An increase in temperature from 440 to 500°C at a feed space velocity of 3.1 g/(g h) leads to an increase in the selectivity from 0.8 to 4.0% for methane, from 5.8 to 12.0% for propylene, and from 7.4 to 43.9% for isobutylene and to a decrease in the acetone selectivity from 61.6 to 12.2%. In this case, the selectivity for ethylene and CO_2 remained almost unchanged (Fig. 5).

Thus, at a temperature of 440°C, the main reaction is the formation of acetone, whereas the contribution of the isobutylene formation reaction is small. An increase in temperature leads to an increase in the contribution of the aldol condensation of acetone to form diacetone alcohol, which further undergoes decomposition to isobutylene, methane, and CO. Thus, an increase in the reaction temperature contributes to an increase in the yield of the desired product, i.e., isobutylene.

Effect of feed space velocity. Figure 5 shows data on the dependence of the product selectivity on the feed space velocity. An increase in the feed space velocity from 1.3 to 3.1 h^{-1} at 500°C does not lead to significant changes in the distribution of products, whereas an increase in the space velocity to 14.5 h^{-1} leads to a marked increase in the acetone selectivity and a decrease in the selectivity for isobutylene, propylene, and methane; this fact suggests that isobutylene, propylene, and methane are formed owing to secondary conversions of acetone, which is consistent with the conversion scheme. At all contact times, $ZnO/8ZrO_2$ exhibited a stable on-stream behavior throughout the entire test.

The highest isobutylene selectivity (43.9 mol %) was observed at a feed space velocity of 3.1 g/(g h); in this case, the isobutylene yield with respect to the theoretical value was 65.8%.

Effect of feedstock composition. Table 3 shows results of studying the effect of the feedstock composition on the parameters of ethanol conversion to isobutylene in the presence of $ZnO/8ZrO_2$ at 500°C, 3.1 g/(g h), and V_{N_2} = 10 mL/min.

With an increase in the ethanol content in the feedstock, the acetone selectivity significantly decreases, because the formation of acetone involves water. In this case, the selectivity for ethylene, propylene, and pentenes increases; these products are apparently formed owing to the isobutylene oligomerization reactions followed by cracking to form propylene and pentenes. Figure 6 shows dependences of the isobutylene yield with respect to the theoretical value on the reaction time for different feedstock compositions in the presence of $ZnO/8ZrO_2$ at 500°C, 3.1 g/(g h), and V_{N_2} = 10 mL/min. The catalyst exhibited a stable on-

Table 2. Ethanol conversion in the presence of ZnO/ZrO_2 at 500°C, 3.1 g/(g h), a 50% ethanol solution, and V_{N_2} = 10 mL/min

Catalyst/Product	ZrO_2	ZnO/ $40ZrO_2$	ZnO/ $20ZrO_2$	ZnO/ $14ZrO_2$	ZnO/ $8ZrO_2$	ZnO/ $6ZrO_2$	ZnO/ $2ZrO_2$
Ethanol conversion, %	100.0	98.6	99.3	99.8	99.9	100.0	92.5
Selectivity for C, mol %							
Methane	3.8	6.9	3.9	4.3	4.0	4.0	2.1
Ethylene	53.6	12.5	4.7	4.0	4.8	2.2	3.5
CO_2	8.7	19.8	20.2	20.8	21.7	19.3	19.3
Propylene	25.1	8.0	12.4	12.3	12.0	8.2	7.7
Acetaldehyde	0.0	0.8	0.1	0.5	0.3	0.0	8.2
Isobutylene	1.2	30.6	48.7	45.2	43.9	29.1	25.8
C_4H_8	0.1	0.0	0.0	0.0	0.0	0.0	0.0
Acetone	6.1	20.4	7.4	11.2	12.2	35.5	32.9
$C_5H_{10} + C_5H_8$	1.1	0.5	1.3	0.8	0.6	0.6	0.0
Other	0.0	0.1	0.0	0.1	0.1	0.1	0.4
Isobutylene yield with respect to theoretical value, %	1.8	45.3	72.6	67.7	65.8	47.3	35.8

stream behavior if the feedstock was a 20 or 50% ethanol solution in water. At a high ethanol content in the feedstock, the catalyst rapidly undergoes deactivation. This finding is apparently attributed to the fact that, in the absence of dilution with water vapors, the resulting isobutylene readily undergoes oligomerization, which leads to a rapid deactivation of the catalyst.

Thus, the best parameters in the synthesis of isobutylene from ethanol were achieved using a 50% ethanol solution in water.

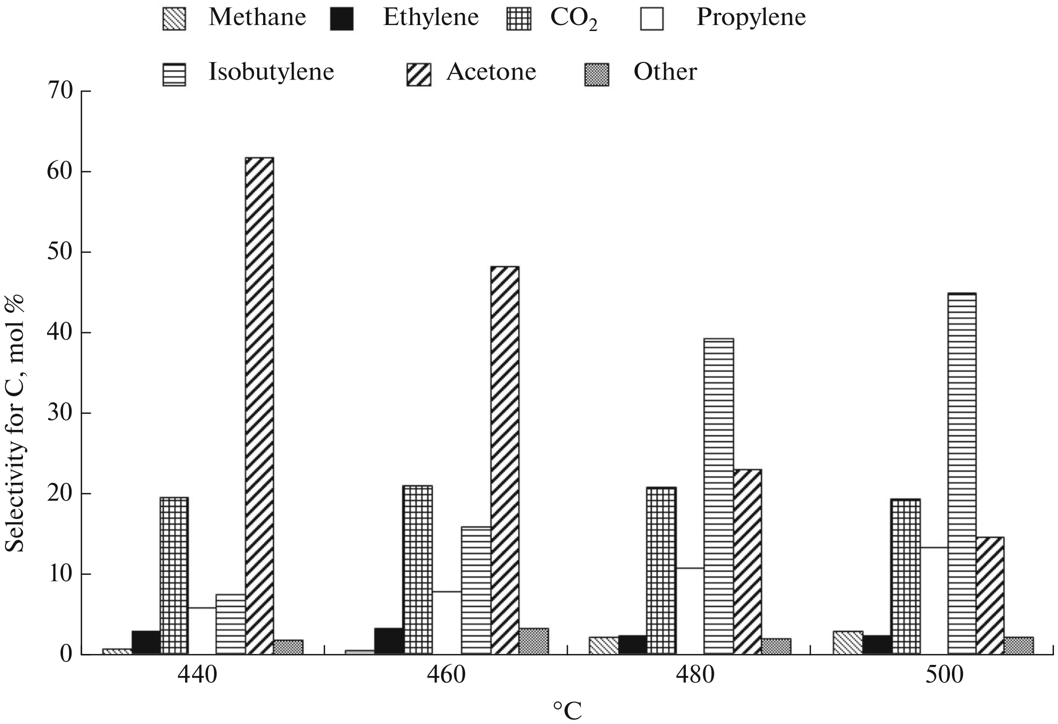

Fig. 4. Temperature dependence of the ethanol conversion product selectivity in the presence of $ZnO/8ZrO_2$ at 3.1 g/(g h), a 50% ethanol solution, and V_{N_2} = 10 mL/min. Ethanol conversion is 100%.

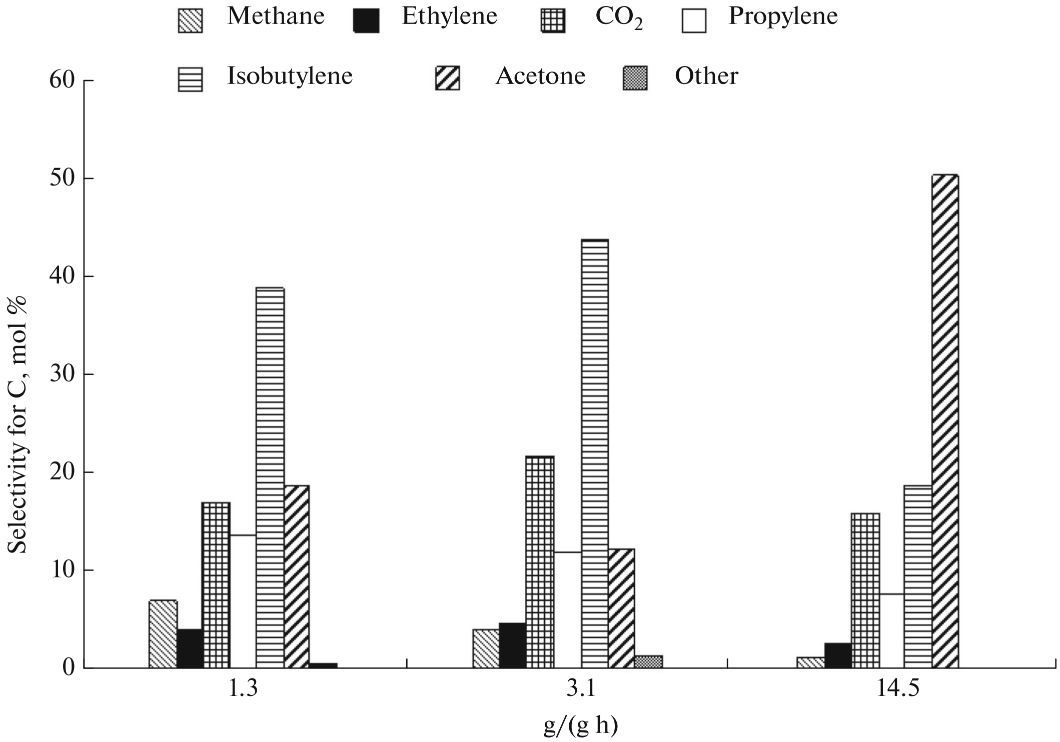

Fig. 5. Dependence of the ethanol conversion product selectivity on the feed space velocity in the presence of $ZnO/8ZrO_2$ at 500°C, a 50% ethanol solution, and V_{N_2} = 10 mL/min. Ethanol conversion is 100%.

Analysis of Deactivated Samples

Table 4 shows data on the weight loss and the peak temperature in the heat flow curves according to TGA–DTA for ZnO/ZrO_2 samples of different compositions after a 3.5-h ethanol conversion reaction at 500°C, 3.1 g/(g h), and V_{N_2} =10 mL/min.

The data suggest that, for all the deactivated samples, the peak temperature in the heat flow curves lies in a temperature range of 300–412°C; the weight loss by the samples in a temperature range of 200–650°C is 1.3–3.0 wt %. The highest weight loss of 3.0 wt % was observed for the $ZnO/40ZrO_2$ sample. These results are consistent with the catalytic test data indicating

Table 3. Ethanol conversion in the presence of $ZnO/8ZrO_2$ at 500°C, 3.1 g/(g h), and V_{N_2} = 10 mL/min

Product/feedstock composition	20% ethanol solution	50% ethanol solution	80% ethanol solution
Ethanol conversion, %	99.7	99.9	99.7
Selectivity for C, mol %			
Methane	3.4	4.0	1.9
Ethylene	1.4	4.8	5.0
CO_2	15.8	21.7	19.2
Propylene	6.3	12.0	21.9
Acetaldehyde	0.1	0.3	0.0
Isobutylene	36.8	43.9	29.1
Acetone	36.1	12.2	16.2
$C_5H_{10} + C_5H_8$	0.0	0.6	4.5
Other	0.0	0.1	2.2
Isobutylene yield with respect to theoretical value, %	55.1	65.8	43.6

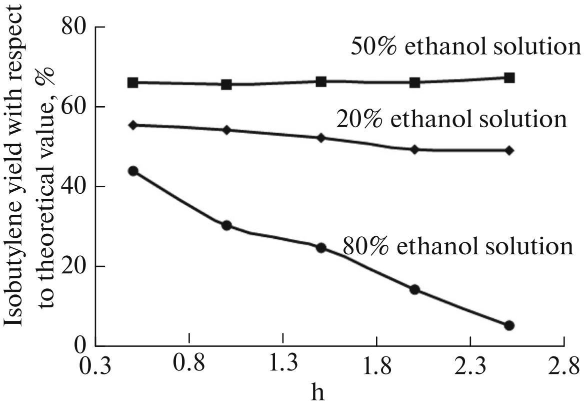

Fig. 6. Dependence of the isobutylene yield with respect to the theoretical value on the reaction time for different feedstock compositions in the presence of $ZnO/8ZrO_2$ at 500°C, 3.1 g/(g h), and V_{N_2} = 10 mL/min.

Table 4. Thermogravimetric and differential thermal analysis of the catalysts after a 3.5-h ethanol conversion reaction at 500°C, 3.1 g/(g h), and V_{N_2} =10 mL/min

Sample	Weight loss in 300–650°C range, wt %	Peak temperature in heat flow curve, °C
$ZnO/2ZrO_2$	1.3	412
$ZnO/6ZrO_2$	1.6	300–368
$ZnO/8ZrO_2$	1.4	379
$ZnO/14ZrO_2$	1.5	357
$ZnO/20ZrO_2$	1.8	376
$ZnO/40ZrO_2$	3.0	357; 402

that the $ZnO/40ZrO_2$ sample undergoes deactivation most rapidly.

Thus, the study of the effect of the catalyst composition and the test conditions has revealed that in order to obtain a catalyst with a high isobutylene selectivity, the Zr : Zn molar ratio in the catalyst should be 8–20, while the optimum conditions for ethanol conversion to isobutylene are 500°C, a feed space velocity of 3 g/(g h), and a feedstock in the form of a 50% ethanol solution in water.

ACKNOWLEDGMENTS

This work was performed under the state task to Topchiev Institute of Petrochemical Synthesis, Russian Academy of Sciences.

REFERENCES

1. V. L. Dagle, C. Smith, M. Flake, et al., Green Chem. **18**, 1880 (2016).
2. V. F. Tret'yakov, Yu. I. Makarfi, K. V. Tret'yakov, et al., Catal. Ind. **2**, 402 (2010).
3. K. K. Ramasamy, M. Gray, H. Job, et al., Catal. Today **269**, 82 (2016).
4. T. A. Phung, L. P. Hernandez, and G. Busca, Appl. Catal., A **489**, 180 (2015).
5. M. Iwamoto, M. Tanaka, S. Hirakawa, et al., ACS Catal. **4**, 3463 (2014).
6. F. Hayashi, M. Tanaka, D. Lin, and M. Iwamoto, J. Catal. **316**, 112 (2014).
7. M. Iwamoto, Catal. Today **242**, 243 (2015).
8. C. Smith, V. L. Dagle, M. Flake, et al., Catal. Sci. Technol. **6**, 2325 (2016).
9. J. Sun, K. Zhu, F. Gao, et al., J. Am. Chem. Soc. **133**, 11096 (2011).
10. J. Sun, R. A. L. Baylon, C. Liu, et al., J. Am. Chem. Soc. **138**, 507 (2016).
11. C. Liu, J. Sun, C. Smith, and Y. Wang, Appl. Catal., A **467**, 91 (2013).
12. B. Zhao, Y. Men, A. Zhang, et al., Appl. Catal., A **558**, 150 (2018).
13. F. Liu, Y. Men, J. Wang, et al., ChemCatChem **9**, 1758 (2017).
14. R. A. L. Baylon, J. Sun, and Y. Wang, Catal. Today **259**, 446 (2016).
15. S. Tayrabekova, P. Maki-Arvela, M. Peurla, et al., Compt. Rend. Chim. (2007). doi 10.1016/j.crci.2017.05.005
16. K. Inui, T. Kurabayashi, and S. Sato, Appl. Catal., A **237**, 53 (2002).
17. J. Sun and Y. Wang, ACS Catal. **4**, 1078 (2014).
18. J. Sun, A. M. Karim, D. Mei, and M. Engelhard, Appl. Catal., B **162**, 141 (2015).
19. C. P. Rodrigues, P. C. Zonetti, C. G. Silva, et al., Appl. Catal., A **458**, 111 (2013).
20. L. R. Silva-Calpa, P. C. Zonetti, D. C. Oliveira, et al., Catal. Today **289**, 264 (2017).
21. S. Letichevsky, P. C. Zonetti, P. P. P. Reis, et al., J. Mol. Catal. A **410**, 177 (2015).
22. B. N. M. van Leeuven, A. M. van der Wulp, I. Duijnstee, et al., Appl. Microbiol. Biotechnol. **93**, 1377 (2012).
23. V. G. Zavodinskii, Perspekt. Mater., No. 2, 5 (2005).

Translated by M. Timoshinina